

Quantitative Evaluation of Weak Nonbonded Se...F Interactions and Their Remarkable Nature as Orbital Interactions

Michio Iwaoka, Hiroto Komatsu, Takayuki Katsuda, and Shuji Tomoda*

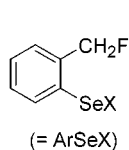
Contribution from the Department of Life Sciences, Graduate School of Arts and Sciences, The University of Tokyo, Komaba, Meguro-ku, Tokyo 153-8902, Japan

Received June 6, 2001. Revised Manuscript Received December 11, 2001

Abstract: To evaluate weak intramolecular nonbonded Se...F interactions recently characterized for a series of *o*-selenobenzyl fluoride derivatives (Iwaoka et al., *Chem. Lett.* **1998**, 969–970), the temperature dependence of the nuclear spin coupling between Se and F ($J_{\text{Se}\cdots\text{F}}$) was investigated for 2-(fluoromethyl)phenylselenenyl cyanate (**1a**) and bis[2-(fluoromethyl)phenyl] diselenide (**1e**) in CD_2Cl_2 and CD_3CN . A significant increase in the magnitude of $J_{\text{Se}\cdots\text{F}}$ was observed for both **1a** and **1e** upon lowering temperature, whereas the values of $J_{\text{Se}\cdots\text{F}}$ for the corresponding trifluoromethyl compounds slightly reduced or remained unchanged at low temperatures. Application of the rapid equilibrium model between two possible conformers revealed that conformer A with an intramolecular Se...F interaction is more stable in enthalpy (ΔH) by 1.23 kcal/mol for **1a** (in CD_2Cl_2) and by 0.85 and 0.83 kcal/mol for **1e** (in CD_2Cl_2 and CD_3CN , respectively) than conformer B, which does not have close Se...F contact. The negligible solvent effects for **1e** suggested marginal electrostatic nature of the Se...F interactions. Instead, importance of the $n_{\text{F}} \rightarrow \sigma_{\text{Se}\cdots\text{X}}^*$ orbital interaction was suggested by quantum chemical (QC) calculations and the natural bond orbital (NBO) analysis.

Introduction

Weak nonbonded interactions¹ play important roles in many chemical phenomena, such as molecular recognition, conformational transformation, and molecular packing in crystals. Although recent progress in experimental methodologies and computational technologies has made studies on weak interactions significantly easier than before, it remains a difficult task in basic chemistry to evaluate them quantitatively.² In this paper, we present the first quantitative estimation of weak nonbonded interactions between selenium and fluorine (Se...F interactions), which have recently been characterized for a series of *o*-selenobenzyl fluoride derivatives (**1**).³ Despite the highest electronegativity of F among main-group elements, it has been found that the Se...F interaction energy for **1e** (X = SeAr) is insensitive to solvent polarity, suggesting that the electrostatic nature may not be important for stability.



- 1a**, X = CN
1b, X = Cl
1c, X = Br
1d, X = SPh
1e, X = SeAr
1f, X = Me
1g, X = B(OMe)₃Na

Nonbonded interactions involving divalent selenium (Se) are intriguing subjects, not only because they have been successfully

applied to asymmetric synthesis⁴ and enzyme-mimetic catalytic reactions⁵ but also because previous experiments have indicated that a pseudo-multivalent state of Se might be related to biological activities of Se compounds.⁶ Moreover, nonbonded interactions involving Se may serve as potential analogues to those involving divalent sulfur, which exists commonly in biomolecules.⁷

We have recently succeeded in evaluation of the weak nonbonded interactions between divalent Se and tertiary amino nitrogen atoms (Se...N interactions) by using a series of *o*-selenobenzylamine derivatives as the model system.⁸ On the basis of variable-temperature ¹H NMR analysis and molecular orbital (MO) calculations, the stabilization energies were estimated as ca. ~5–20 kcal/mol depending on the property of the substituent at Se. It was concluded that the Se...N interactions are mostly stabilized by the orbital interaction between the nitrogen lone pair (n_{N}) and the low-lying antibonding orbital

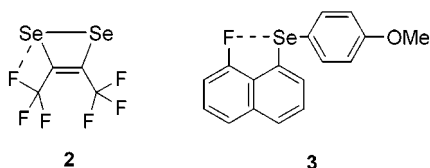
- (2) Müller-Dethlefs, K.; Hobza, P. *Chem. Rev.* **2000**, *100*, 143–167.
 (3) Iwaoka, M.; Komatsu, H.; Tomoda, S. *Chem. Lett.* **1998**, 969–970.
 (4) (a) Fujita, K.; Iwaoka, M.; Tomoda, S. *Chem. Lett.* **1994**, 923–926. (b) Fujita, K.; Murata, K.; Iwaoka, M.; Tomoda, S. *Tetrahedron* **1997**, *53*, 2029–2048. (c) Wirth, T. *Liebigs Ann./Recl.* **1997**, 2189–2196. (d) Spichty, M.; Fragale, G.; Wirth, T. *J. Am. Chem. Soc.* **2000**, *122*, 10914–10916.
 (5) (a) Iwaoka, M.; Tomoda, S. *J. Chem. Soc., Chem. Commun.* **1992**, 1165–1167. (b) Wirth, T.; Häuptli, S.; Leuenberger, M. *Tetrahedron: Asymm.* **1998**, *9*, 547–550.
 (6) (a) Iwaoka, M.; Tomoda, S. *J. Am. Chem. Soc.* **1994**, *116*, 2557–2561. (b) Mughesh, G.; Singh, H. B. *Chem. Soc. Rev.* **2000**, *29*, 347–357. (c) Mughesh, G.; Panda, A.; Singh, H. B.; Punekar, N. S.; Butcher, R. J. *J. Am. Chem. Soc.* **2001**, *123*, 839–850.
 (7) (a) Nagao, Y.; Hirata, T.; Goto, S.; Sano, S.; Kakehi, A.; Iizuka, K.; Shiro, M. *J. Am. Chem. Soc.* **1998**, *120*, 3104–3110. (b) Wu, S.; Greer, A. J. *Org. Chem.* **2000**, *65*, 4883–4887. (c) Iwaoka, M.; Takemoto, S.; Okada, M.; Tomoda, S. *Chem. Lett.* **2001**, 132–133.
 (8) Iwaoka, M.; Tomoda, S. *J. Am. Chem. Soc.* **1996**, *118*, 8077–8084.

* To whom correspondence should be addressed: Phone +81 (3) 5454-6575; fax +81 (3) 5454-6998; e-mail tomoda@selen.c.u-tokyo.ac.jp.

(1) (a) Israelachvili, J. *Intermolecular and Surface Forces*; Academic Press: London, 1991. (b) *Molecular Interactions*; Scheiner, S., Ed.; John Wiley and Sons: Chichester, U.K., 1997.

of Se ($\sigma_{\text{Se-X}}^*$). On the other hand, two mutually different stabilization mechanisms (i.e., electrostatic and orbital interaction mechanisms) were reported for intramolecular nonbonded Se...O interactions by Goldstein et al.⁹ and Barton et al.,¹⁰ respectively, depending on the model systems. Our systematic examination using *o*-selenobenzaldehyde and *o*-selenobenzyl alcohol derivatives suggested that the Se...O interactions are weaker than the corresponding Se...N interactions and that an orbital interaction mechanism is still a dominant factor for the stability.¹¹ The strong interaction between a cationic Se and an alcoholic O atom (the Se⁺...O interaction) was also extensively analyzed in relation to selenium-based asymmetric syntheses.^{4d}

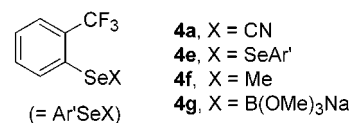
Nonbonded Se...F interaction is an extreme case to test the electrostatic character of divalent Se, since F is the most electronegative main-group element in the periodic table. Although several compounds were found to have close Se...F contacts in the solid state,¹² mechanistic studies of the Se...F interactions appeared only recently. Borisenko et al.¹³ suggested the electrostatic nature of the Se...F interaction observed for **2** in the gas phase. On the other hand, Nakanishi et al.¹⁴ discussed orbital interactions of the close Se...F contact in **3**. These compounds, however, possess strong steric restrictions, hence the intrinsic nature of weak Se...F interaction is not yet thoroughly elucidated.



Se...F interaction can also serve as a useful probe for estimating the electron-donating character of organic fluorides, since it was previously shown by the studies of nonbonded Se...N and Se...O interactions that Se is a good electron acceptor.^{8,11} Although F is a strong σ electron-withdrawing element, an electron-donating character of F lone pairs has often been pointed out.¹⁵ Evaluation and mechanistic characterization of Se...F interaction is therefore of significant interest from the viewpoint of organic fluorine chemistry.

The main purposes of this paper are 3-fold: (1) to estimate the stabilization energies of weak nonbonded Se...F interactions in various solvents, (2) to delineate the stabilization mechanism of Se...F interactions, i.e., to assess relative importance of orbital

and electrostatic characters, and (3) to show usefulness of the combined method of quantum chemical (QC) calculations and natural bond orbital (NBO) analysis to understand these weak interactions. We took advantage of a series of *o*-selenobenzyl fluoride derivatives (**1**) as model compounds, which have the freedom of internal rotation to adopt or to avoid intramolecular Se...F contact. In addition, the corresponding trifluoromethyl (CF₃) compounds (**4**) were employed as references because they always adopt intramolecular Se...F contact independent of the internal rotation of the C–CF₃ bond. Our preliminary investigations with this model system have already shown the presence of nonbonded Se...F interactions for **1** in CDCl₃.³ The proposed $n_{\text{F}} \rightarrow \sigma_{\text{Se-X}}^*$ orbital interaction mechanism was theoretically supported by Jeong and Kwon recently.¹⁶ Here, we have developed a novel methodology to evaluate weak Se...F interactions by using the temperature dependence of $J_{\text{Se...F}}$. The stabilization mechanisms are discussed on the basis of the observed solvent effects on the interaction energies as well as on the basis of the results from QC and NBO analyses.



Results and Discussion

Model Compounds. A series of *o*-selenobenzyl fluorides (**1a–g**) were synthesized as model compounds to investigate intramolecular nonbonded Se...F interactions. Diselenide **1e** was synthesized from bis[2-(chloromethyl)phenyl] diselenide¹⁷ by applying modified Ichihara's fluorination method,¹⁸ in which butyronitrile was used as a solvent instead of acetonitrile in order to raise the reaction temperature. Compound **1e** was then converted into the other model compounds (**1a–d** and **1f,g**) by using the common procedures.^{3,8} Compounds were identified with ¹H, ¹³C, ¹⁹F, and ⁷⁷Se NMR spectra, although **1b** was contaminated by small amounts of **1e** and an unknown byproduct, and **1d** slowly disproportionated into **1e** and diphenyl disulfide at room temperature.

Similar procedures were employed for the synthesis of the corresponding CF₃ compounds (**4**). Selenocyanate **4a** was synthesized from *o*-trifluoromethylaniline by diazotization, followed by treatment with potassium selenocyanate. Compound **4a** was then converted into **4e** and **4f**. Selenolate **4g** was prepared in situ by treatment of **4e** with sodium borohydride in CD₃OD.¹⁹ All reference compounds were also characterized spectrally.

NMR Chemical Shifts and $J_{\text{Se...F}}$ Coupling Constants. ⁷⁷Se NMR chemical shifts (δ_{Se}), ¹⁹F NMR chemical shifts (δ_{F}), and nuclear spin coupling constants between ⁷⁷Se and ¹⁹F ($J_{\text{Se...F}}$) observed for **1a–g**, **4a**, **4e**, and **4g** at 298 K were tabulated previously (Table 1 of ref 3). Nonbonded Se...F interactions of **1a–f** have been characterized as follows.

Unexpectedly large $J_{\text{Se...F}}$ coupling constants were observed for **1a–f** ($J_{\text{Se...F}} = \sim 22.7\text{--}84.2$ Hz in CDCl₃).³ Because ⁴ $J_{\text{Se–F}}$

- (9) (a) Goldstein, B. M.; Kennedy, S. D.; Hennen, W. J. *J. Am. Chem. Soc.* **1990**, *112*, 8265–8268. (b) Burling, F. T.; Goldstein, B. M. *J. Am. Chem. Soc.* **1992**, *114*, 2313–2320.
 (10) Barton, D. H. R.; Hall, M. B.; Lin, Z. Y.; Parekh, S. I.; Reibenspies, J. J. *Am. Chem. Soc.* **1993**, *115*, 5056–5059.
 (11) Komatsu, H.; Iwaoka, M.; Tomoda, S. *Chem. Commun.* **1999**, 205–206.
 (12) (a) Gallois, B.; Gaultier, J.; Hauw, C.; Lamcharfi, T.-D.; Filhol, A. *Acta Crystallogr.* **1986**, *B42*, 564–575. (b) Emge, T. J.; Wang, H. H.; Beno, M. A.; Williams, J. M.; Whangbo, M.-H.; Evain, M. *J. Am. Chem. Soc.* **1986**, *108*, 8215–8223.
 (13) Borisenko, K. B.; Broschag, M.; Hargittai, I.; Klapötke, T. M.; Schröder, D.; Schulz, A.; Schwarz, H.; Tornieporth-Oetting, I. C.; White, P. S. *J. Chem. Soc., Dalton Trans.* **1994**, 2705–2712.
 (14) Nakanishi, W.; Hayashi, S.; Sakaue, A.; Ono, G.; Kawada, Y. *J. Am. Chem. Soc.* **1998**, *120*, 3635–3640.
 (15) (a) Tomoda, S.; Takamatsu, K.; Iwaoka, M. *Chem. Lett.* **1998**, 581–582. (b) Jefford, C. W.; Hill, D. T.; Ghosez, L.; Toppet, S.; Ramey, K. C. *J. Am. Chem. Soc.* **1969**, *91*, 1532–1534. (c) Yamamoto, G.; Oki, M. *J. Org. Chem.* **1984**, *49*, 1913–1917. (d) Yamamoto, G.; Oki, M. *Tetrahedron Lett.* **1985**, *26*, 457–460. (e) Gribble, G. W.; Kelly, W. J. *Tetrahedron Lett.* **1985**, *26*, 3779–3782. (f) Dunitz, J. D.; Taylor, R. *Chem. Eur. J.* **1997**, *3*, 89–98. (g) Plenio, H. *Chem. Rev.* **1997**, *97*, 3363–3384. (h) Thalladi, V. R.; Weiss, H.-C.; Bläser, D.; Boese, R.; Nangia, A.; Desiraju, G. R. *J. Am. Chem. Soc.* **1998**, *120*, 8702–8710.

- (16) Jeong, M.; Kwon, Y. *Chem. Phys. Lett.* **2000**, *328*, 509–515.
 (17) Iwaoka, M.; Tomoda, S. *Phosphorus Sulfur Silicon Relat. Elem.* **1992**, *67*, 125–130.
 (18) Ichihara, J.; Matsuo, T.; Hanafusa, T.; Ando, T. *J. Chem. Soc., Chem. Commun.* **1986**, 793–794.
 (19) Miyashita, M.; Hoshino, M.; Yoshikoshi, A. *Tetrahedron Lett.* **1988**, *29*, 347–350.

Table 1. $J_{\text{Se}\cdots\text{F}}$ Coupling Constants Observed for **1a**, **1e**, and **1f** in Various NMR Solvents at 298 K

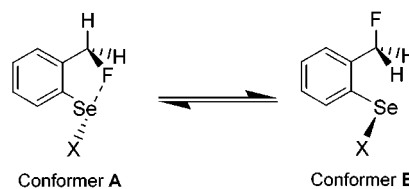
solvent	ϵ^a	$J_{\text{Se}\cdots\text{F}}^b$ (Hz)		
		1a (X = CN)	1e (X = SeAr)	1f (X = Me)
(CD ₃) ₂ S=O	46.45	39.0	32.6	29.4
CD ₃ CN	35.94	62.9	30.3	27.1
(CD ₃) ₂ C=O	20.56	68.7	30.0	26.2
CD ₂ Cl ₂	8.93	76.9	24.7	23.9
CDCl ₃	4.81	84.2	23.6	22.7
C ₆ D ₆	2.27	81.8	23.0	22.1

^a Dielectric constants of the solvents at 298 K quoted from ref 21. ^bThe values of $J_{\text{Se}\cdots\text{F}}$ coupling constants were measured from the expanded ¹H-decoupled ⁷⁷Se NMR spectra.

coupling constants are usually small [$^4J_{\text{Se}-\text{F}} = \sim 10\text{--}28$ Hz for 2,4,6-tris(trifluoromethyl)phenylseleno derivatives],²⁰ the larger values of $J_{\text{Se}\cdots\text{F}}$ for **1a–f** suggested the presence of direct through-space nonbonded interactions between Se and F. The magnitude of $J_{\text{Se}\cdots\text{F}}$ correlated positively with the downfield shifts of δ_{F} , except for **1c** (X = Br).³ The propensity suggested that the F atom loses more electrons as the Se \cdots F interaction becomes stronger. Therefore, the electrons may delocalize from F to Se in the Se \cdots F interactions. The $J_{\text{Se}\cdots\text{F}}$ coupling was not detected for selenolate **1g** ($J_{\text{Se}\cdots\text{F}} = 0$ Hz in CD₃OD), in which the excessive negative charge at Se may cause repulsion with the F lone pair electrons to avoid close Se \cdots F contact. Consequently, the $J_{\text{Se}\cdots\text{F}}$ coupling could be observed only when nonbonded Se \cdots F interaction existed in solution.

Table 1 shows solvent effects on $J_{\text{Se}\cdots\text{F}}$ observed for **1a** (X = CN), **1e** (X = SeAr), and **1f** (X = Me) at room temperature. The value of $J_{\text{Se}\cdots\text{F}}$ for **1a** decreased significantly with an increasing dielectric constant of the solvents,²¹ while completely opposite trends were observed for **1e** and **1f**. Since the cyano group is a strong electron-withdrawing substituent, the Se \cdots F interaction of **1a** would possess electrostatic character to some extent. Hence the interaction might become weaker in polar solvents. Similar electrostatic contribution was previously found for the nonbonded Se \cdots N interaction of *N,N*-dialkyl-2-(aminomethyl)phenylselenenyl cyanate.⁸ On the other hand, remarkable enhancement of $J_{\text{Se}\cdots\text{F}}$ in polar solvents observed for **1e** and **1f** suggested that the electrostatic character of the Se \cdots F interactions in this system may be negligible. The result is quite surprising considering the high electronegativity of F.

Rapid Equilibrium between Conformers A and B. ⁷⁷Se NMR signals of reference compounds appeared as quartets ($J_{\text{Se}\cdots\text{F}} = 63.2$ Hz for **4a**, 53.0 Hz for **4e**, 48.4 Hz for **4f**, and 15.6 Hz for **4g**), indicating free rotation of the CF₃ groups at room temperature. In addition, low-temperature ¹H NMR spectra of **1a–f** showed a sharp singlet in the region of benzylic protons even at -90 °C at 500 MHz. To explain the dynamic NMR spectra, rapid equilibrium between two stable conformers has been proposed (Figure 1):³ Conformer A has close atomic contact between Se and F with almost linear X–Se \cdots F atomic alignment, and conformer B has the C–F bond away from the Se–X bond, which lies out of the aromatic plane.

**Figure 1.** Equilibrium between two stable conformers (A and B) of **1**.

By use of the rapid equilibrium model (Figure 1), it is possible to evaluate the Se \cdots F interaction energies ($H_{\text{Se}\cdots\text{F}}$) experimentally as follows. First, the observed value of $J_{\text{Se}\cdots\text{F}}$ represents weighted average of those for conformers A and B:

$$J_{\text{Se}\cdots\text{F}} = J_{\text{Se}\cdots\text{F}}(\text{A})\chi_{\text{A}} + J_{\text{Se}\cdots\text{F}}(\text{B})(1 - \chi_{\text{A}}) \quad (1)$$

where $J_{\text{Se}\cdots\text{F}}(\text{A})$ and $J_{\text{Se}\cdots\text{F}}(\text{B})$ are the Se \cdots F coupling constants for conformers A and B, respectively. χ_{A} is a temperature-dependent variable representing the relative population of conformer A. It should be noted that the value of $J_{\text{Se}\cdots\text{F}}(\text{B})$ for **1a–f** would be approximately zero [$J_{\text{Se}\cdots\text{F}}(\text{B}) \approx 0$ Hz; namely, $J_{\text{Se}\cdots\text{F}} \approx J_{\text{Se}\cdots\text{F}}(\text{A})\chi_{\text{A}}$] because the nuclear spin coupling between Se and F was not observed for **1g**, for which conformer B is predicted to be the only stable conformer in solution. Second, χ_{A} is related to enthalpy and entropy changes (ΔH and ΔS) of the equilibrium (Figure 1) by the free energy relationship:

$$\Delta G = \Delta H - T\Delta S = -RT \ln \{(1 - \chi_{\text{A}})/\chi_{\text{A}}\} \quad (2)$$

where T and R represent temperature and the gas constant, respectively. Third, since rotational barriers of the CH₂F group and the Se–X moiety must be low as indicated by the low-temperature NMR spectra, the enthalpy for the interaction between Se and F ($H_{\text{Se}\cdots\text{F}}$) is approximately equal to ΔH :

$$H_{\text{Se}\cdots\text{F}} \approx \Delta H \quad (3)$$

Thus, in principle a quantitative estimate of $H_{\text{Se}\cdots\text{F}}$ can be experimentally determined by measuring $J_{\text{Se}\cdots\text{F}}$ values at various temperatures if $J_{\text{Se}\cdots\text{F}}(\text{A})$ remains constant. This critical condition was practically examined by using the $J_{\text{Se}\cdots\text{F}}$ values for the corresponding CF₃ compounds (**4**) at various temperatures.

Temperature Dependence of $J_{\text{Se}\cdots\text{F}}$ for **1a and **1e**.** Compounds **1a** (X = CN) and **1e** (X = SeAr) were selected to investigate the temperature dependence of $J_{\text{Se}\cdots\text{F}}$ because they are remarkably more stable than the other model compounds. CD₃CN and CD₂Cl₂ were selected as polar and less polar solvents, respectively. The values of $J_{\text{Se}\cdots\text{F}}$ were measured from the expanded ⁷⁷Se NMR spectra, in which the signals are split into a doublet due to coupling with the nuclear spin of ¹⁹F. As seen in Figure 2, the splitting of ⁷⁷Se NMR signals was enhanced at low temperatures in CD₂Cl₂ for both **1a** and **1e**. Similar propensities were also observed in CD₃CN. The $J_{\text{Se}\cdots\text{F}}$ vs T plots for **1a** and **1e** are shown in Figures 3 and 4, respectively, where the data for the reference compounds (**4a** and **4e**) are also plotted.

Figure 3 suggests two important features as to the Se \cdots F interaction of **1a** (the NC–Se \cdots F interaction). First, the Se \cdots F interaction is attractive in both solvents ($H_{\text{Se}\cdots\text{F}} > 0$). This can be predicted as follows. According to the rapid equilibrium model (Figure 1 and eq 1), the increase of the magnitude of $J_{\text{Se}\cdots\text{F}}$ observed for **1a** at low temperatures should be due to the enhancement of χ_{A} or $J_{\text{Se}\cdots\text{F}}(\text{A})$. However, the $J_{\text{Se}\cdots\text{F}}(\text{A})$ value

(20) (a) Bertel, N.; Roesky, H. W.; Edelmann, F. T.; Noltemeyer, M.; Schmidt, H. G. *Z. Anorg. Chem.* **1990**, *586*, 7–18. (b) Labahn, D.; Bohnen, F. M.; Herbst-Irmer, R.; Pohl, E.; Stalke, D.; Roesky, H. W. *Z. Anorg. Allg. Chem.* **1994**, *620*, 41–47.

(21) *Techniques of Chemistry*; Riddick, J. A., Bunger, W. B., Sakano, T. K., Eds.; John Wiley and Sons: New York, 1986; Vol. 2.

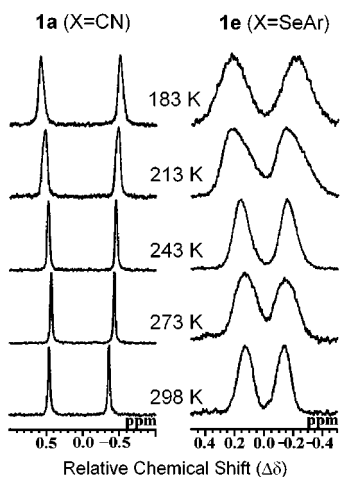


Figure 2. ^{77}Se NMR spectra (95.35 MHz) observed for **1a** (left panel) and **1e** (right panel) in CD_2Cl_2 at various temperatures.

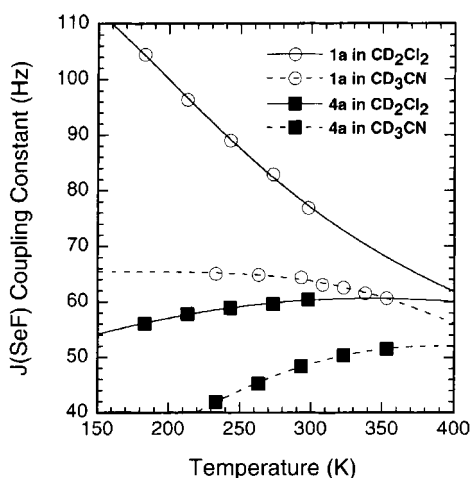


Figure 3. Plots of $J_{\text{Se}\cdots\text{F}}$ observed for **1a** (O) and **4a** (9) in CD_2Cl_2 and CD_3CN as a function of temperature. The solid curve (in CD_2Cl_2) for **1a** was depicted with the parameters obtained by data fitting. The other curves were drawn for convenience with no physical meaning.

for **1a** must be reduced slightly at low temperatures because the $J_{\text{Se}\cdots\text{F}}$ value for the reference compound (**4a**) decreased with lowering the temperature. Therefore, the equilibrium would proceed toward conformer A at low temperatures. Second, the NC–Se...F interaction is affected by polarity of the solvent employed. The values of $J_{\text{Se}\cdots\text{F}}$ for both **1a** and **4a** were smaller in CD_3CN than those in CD_2Cl_2 . This is probably due to stronger solvation by CD_3CN than that by CD_2Cl_2 . The observed decrease in the $J_{\text{Se}\cdots\text{F}}$ value for **4a** at low temperatures can also be ascribed to the effects of solvation because the solvation would slightly weaken the Se...F interaction by reducing the net charge of the electrophilic Se atom.

On the other hand, different behaviors were observed for **1e**. As seen in Figure 4, the value of $J_{\text{Se}\cdots\text{F}}$ for **1e** significantly increased with lowering the temperature in both CD_3CN and CD_2Cl_2 , whereas that for **4e** remained constant. The constant value of $J_{\text{Se}\cdots\text{F}}$ for **4e** suggested that the value of $J_{\text{Se}\cdots\text{F}}(\text{A})$ for **1e** is independent of temperature in both solvents. Therefore, the observed increase of the $J_{\text{Se}\cdots\text{F}}$ value for **1e** should be directly due to the enhancement of the relative population of conformer A (χ_{A}) at low temperatures. This implies that the nonbonded Se...F interaction of **1e** (the Se–Se...F interaction) may be attractive. Furthermore, the values of $J_{\text{Se}\cdots\text{F}}$ in CD_2Cl_2 for **1e**

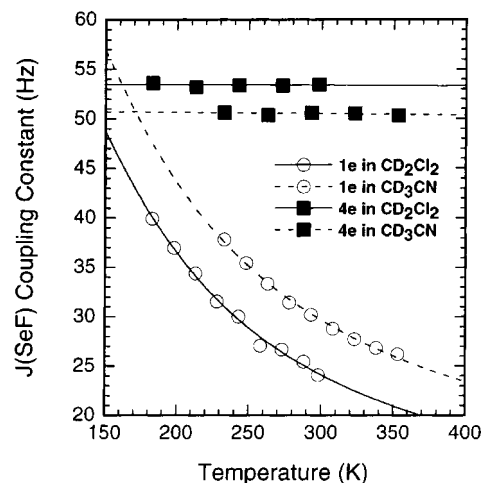


Figure 4. Plots of $J_{\text{Se}\cdots\text{F}}$ observed for **1e** (O) and **4e** (9) in CD_2Cl_2 and CD_3CN as a function of temperature. The solid (in CD_2Cl_2) and dashed (CD_3CN) curves for **1e** were depicted with the parameters obtained by data fitting.

and **4e** were unexpectedly not much different from those in CD_3CN . The observation again suggested that the Se...F interaction should not have much electrostatic character.

The solvent effect on $J_{\text{Se}\cdots\text{F}}$ observed for **1a** was different from that for **1e** as discussed above. The discrepancy may be due to the preferential solvation at the SeCN moiety of **1a**, unlike the CH_2F moiety of **1a**, since only a marginal solvent effect was observed for **1e**. This is consonant with the hydrophobicity of organic fluorides.²²

Evaluation of Se...F Interaction Energies ($H_{\text{Se}\cdots\text{F}}$). By fitting the temperature-dependent $J_{\text{Se}\cdots\text{F}}$ data obtained for **1a** and **1e** to eqs 1–3, stabilization energies of the nonbonded Se...F interactions ($H_{\text{Se}\cdots\text{F}}$) were evaluated.

For the case of **1e** (the Se–Se...F interaction), the fitting was straightforward since the value of $J_{\text{Se}\cdots\text{F}}(\text{A})$ should be constant at various temperatures as suggested by the constant value of $J_{\text{Se}\cdots\text{F}}$ for **4e**. The values of $H_{\text{Se}\cdots\text{F}}$ for **1e** were estimated as 0.85 ± 0.20 kcal/mol in CD_2Cl_2 and 0.83 ± 0.22 kcal/mol in CD_3CN . Thus, negligible solvent effects were quantitatively confirmed. The interaction energies determined were significantly smaller than those previously estimated for Se...N interactions (~ 5 – 20 kcal/mol)⁸ due to the lower nucleophilicity of F than N. The values of ΔS and $J_{\text{Se}\cdots\text{F}}(\text{A})$, which were simultaneously converged, were 4.2 ± 0.2 eu and 73 ± 21 Hz, respectively, in CD_2Cl_2 and 3.9 ± 0.6 eu and 81 ± 33 Hz, respectively, in CD_3CN . The positive values of ΔS were consistent with the larger conformational flexibility of conformer B.

On the other hand, the data fitting was difficult for the case of **1a** because the value of $J_{\text{Se}\cdots\text{F}}(\text{A})$ should not be constant at low temperatures, as suggested by the decrease of $J_{\text{Se}\cdots\text{F}}$ observed for **4a**. However, it may be a reasonable assumption in CD_2Cl_2 that the value of $J_{\text{Se}\cdots\text{F}}(\text{A})$ for **1a** is approximately constant because the $J_{\text{Se}\cdots\text{F}}$ values for **4a** decreased only slightly and the $J_{\text{Se}\cdots\text{F}}$ value for **1a** increased greatly with lowering temperature. On the basis of this hypothesis, the NC–Se...F interaction energy ($H_{\text{Se}\cdots\text{F}}$) of **1a** was estimated as 1.23 ± 0.18

(22) *Organofluorine Compounds in Medicinal Chemistry and Biomedical Applications*; Filler, R., Kobayashi, Y., Yagupolskii, L. M., Eds.; Elsevier: Amsterdam, 1993.

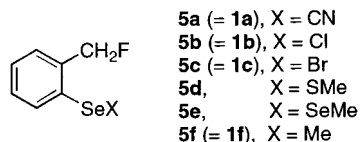
Table 2. Summary of Quantum Chemical (QC) Calculations on **5a–f** and the Natural Bond Orbital (NBO) Analysis

compd	method ^a	ΔE_{AB}^b (kcal/mol)	$r_{Se...F}^c$ (Å)	$\angle F...Se-X^c$ (deg)	ω_{Ar-C}^c (deg)	ΔE_{del}^d (kcal/mol)	Δq_{Se}^e (e ⁻)	Δq_F^f (e ⁻)
5a	I	-1.1	2.92	160.6	54.2	3.5	0.0048	-0.0076
	II	-1.2	2.79	168.8	49.4			
5b	I	+0.1	2.97	155.6	56.2	3.0	0.0045	-0.0073
	II	-0.5	2.69	170.7	47.0			
5c	I	+1.3	3.25	133.4	67.0	1.0	0.0010	-0.0025
	II	-1.1	2.76	168.6	51.2			
5d	I	+0.1	3.08	159.4	60.8	2.1	0.0027	-0.0050
	II	-0.0	2.91	171.6	54.2			
5e	I	+0.7	3.10	158.0	62.7	2.0	0.0024	-0.0046
	II	+0.2	2.94	171.4	55.9			
5f	I	+0.3 (+0.2) ^g	3.14	157.6	62.9	1.6	0.0024	-0.0046
	II	-0.2 (+0.0) ^g	2.99	169.6	58.1			

^a QC calculations were carried out at the B3LYP/6-31G(d,p)//HF/6-31G(d,p) level (method I) and the B3LYP/6-31G(d,p)//B3LYP/6-31G(d,p) level (method II) by use of Huzinaga's 43321/4321/311 basis sets for Se and Br. NBO analysis was performed at the HF/6-31G(d,p) level. ^b Energy of conformer A relative to that of conformer B, corrected with the unscaled zero-point energies. ^c Selected structural parameters obtained for conformer A. ω_{Ar-C} is the dihedral angle along the Ar-CH₂F bond. ^d Total stabilization energy due to the orbital interactions between SeX and F for conformer A revealed by the NBO deletion analysis. ^e Change of the electron population for the $\sigma_{Se...X}^*$ orbital due to the Se...F orbital interaction of conformer A. ^f Change of the electron population for the n_F orbitals due to the Se...F orbital interaction of conformer A. ^g Energy of conformer A relative to that of conformer C.

kcal/mol in CD₂Cl₂. The simultaneously converged values of ΔS and $J_{Se...F}(A)$ were 2.9 ± 0.4 eu and 120 ± 5 Hz, respectively. The estimated Se...F interaction energy for **1a** (1.23 kcal/mol) was 0.38 kcal/mol larger than that for **1e** (0.85 kcal/mol) in the same solvent, being consistent with the higher electrophilicity of selenocyanates than diselenides. For the data obtained in CD₃CN, such a fitting could not be applied because of larger solvent effects: the Se...F interaction should be weaker than 1.23 kcal/mol because solvation around the SeCN moiety may attenuate the Se...F atomic contact.

QC Calculations and the NBO Analysis. To rationalize the experimental results, QC calculations were carried out on **5a–f**, two of which have a simplified substituent at Se to save computational time. Gaussian 94 and 98 programs^{23,24} were used for all calculations. Structures were fully optimized at the HF/6-31G(d,p) or B3LYP/6-31G(d,p) level by use of Huzinaga's 43321/4321/311 basis sets²⁵ for Se and Br. Single-point energies were subsequently calculated at the level of the density functional theory (B3LYP).²⁶ To analyze the mechanism of the observed nonbonded Se...F interactions, NBO analysis of Weinhold and co-workers²⁷ was performed.



Three to six possible conformers were located for **5a–f**: two corresponded to conformers A and B (Figure 1), and the others included an unstable conformer with both the C–F and Se–X bonds tilted out of the aromatic plane to the same direction (conformer C), one with both the C–F and Se–X bonds lying on the aromatic plane, etc. Except for **5f**, the energies of conformers A and B were found to be obviously lower than those of the other conformers. Therefore, we consider only the

two stable conformers in the following discussion. For the case of **5f** (X = Me), the most stable conformer was found to be conformer C at the B3LYP/6-31G(d,p)//B3LYP/6-31G(d,p) level. Hence, three conformers are considered for **5f**. The results of QC calculations and the NBO analysis are summarized in Table 2.

For all compounds, energies of conformers A and B were close to each other ($\Delta E_{AB} = -1.2$ to $+1.3$ kcal/mol), suggesting that both conformers may exist in solution. Thus, the fitting analysis of the NMR data based on a rapid equilibrium model (Figure 1) could be rationalized. The values of ΔE_{AB} for **5a** ($\Delta E_{AB} = -1.1$ and -1.2 kcal/mol in methods I and II, respectively) were in excellent agreement with the Se...F interaction energy experimentally estimated for **1a** in CD₂Cl₂ ($H_{Se...F} = 1.23 \pm 0.18$ kcal/mol). Therefore, it was strongly suggested that solvent effect on the Se...F interaction, and hence the electrostatic character, is insignificant. On the other hand, the values of ΔE_{AB} for **5e** ($\Delta E_{AB} = +0.7$ and $+0.2$ kcal/mol in methods I and II, respectively) were a little different from those estimated for **1e** ($H_{Se...F} = 0.85 \pm 0.20$ and 0.83 ± 0.22 kcal/mol in CD₂Cl₂ and CD₃CN, respectively). This is probably due to the simplified molecular structure of **5e** compared with **1e**.

The effect of electron correlation on the Se...F interactions is obviously seen in Table 2. Comparing the Se...F nonbonded distance ($r_{Se...F}$) of conformer A optimized at the HF/6-31G(d,p) level (method I) with those optimized at the B3LYP/6-31G(d,p) level (method II), it was revealed that more accurate treatment of electron correlation causes strengthening of the Se...F interaction for **5a–f**. The most remarkable change was

(23) Frisch, M. J.; Trucks, G. W.; Schlegel, H. B.; Gill, P. M. W.; Johnson, B. G.; Robb, M. A.; Cheeseman, J. R.; Keith, T.; Petersson, G. A.; Montgomery, J. A.; Raghavachari, K.; Al-Laham, M. A.; Zakrzewski, V. G.; Ortiz, J. V.; Foresman, J. B.; Cioslowski, J.; Stefanov, B. B.; Nanayakkara, A.; Challacombe, M.; Peng, C. Y.; Ayala, P. Y.; Chen, W.; Wong, M. W.; Andres, J. L.; Replogle, E. S.; Gomperts, R.; Martin, R. L.; Fox, D. J.; Binkley, J. S.; Defrees, D. J.; Baker, J.; Stewart, J. P.; Head-Gordon, M.; Gonzalez, C.; Pople, J. A. *Gaussian 94*; Gaussian, Inc.: Pittsburgh, PA, 1995.

(24) Frisch, M. J.; Trucks, G. W.; Schlegel, H. B.; Scuseria, G. E.; Robb, M. A.; Cheeseman, J. R.; Zakrzewski, V. G.; Montgomery, J. A.; Stratmann, R. E.; Burant, J. C.; Dapprich, S.; Millam, J. M.; Daniels, A. D.; Kudin, K. N.; Strain, M. C.; Farkas, O.; Tomasi, J.; Barone, V.; Cossi, M.; Cammi, R.; Mennucci, B.; Pomelli, C.; Adamo, C.; Clifford, S.; Ochterski, J.; Petersson, G. A.; Ayala, P. Y.; Cui, Q.; Morokuma, K.; Malick, D. K.; Rabuck, A. D.; Raghavachari, K.; Foresman, J. B.; Cioslowski, J.; Ortiz, J. V.; Baboul, A. G.; Stefanov, B. B.; Liu, G.; Liashenko, A.; Piskorz, P.; Komaromi, I.; Gomperts, R.; Martin, R. L.; Fox, D. J.; Keith, T.; Al-Laham, M. A.; Peng, C. Y.; Nanayakkara, A.; Gonzalez, C.; Challacombe, M.; Gill, P. M. W.; Johnson, B.; Chen, W.; Wong, M. W.; Andres, J. L.; Gonzalez, C.; Head-Gordon, M.; Replogle, E. S.; Pople, J. A. *Gaussian 98*; Gaussian, Inc.: Pittsburgh, PA, 1998.

(25) *Gaussian Basis Sets for Molecular Calculations*; Huzinaga, S., Ed.; Elsevier: Amsterdam, 1984.

(26) (a) Lee, C.; Yang, W.; Parr, R. G. *Phys. Rev. B* **1988**, *37*, 785–789. (b) Becke, A. D. *J. Chem. Phys.* **1993**, *98*, 5648–5652.

(27) Reed, A. E.; Curtiss, L. A.; Weinhold, F. *Chem. Rev.* **1988**, *88*, 899–926.

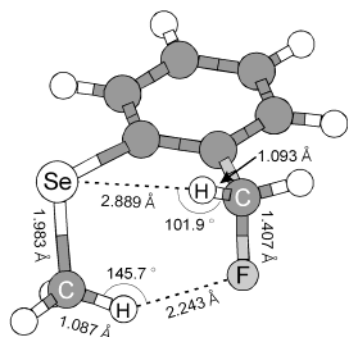


Figure 5. Molecular structure of conformer C obtained for **5f** (X = Me) at the B3LYP/6-31G(d,p) level by use of Huzinaga's 43321/4321/311 basis sets for Se.

observed for **5c** (X = Br): The value of $r_{\text{Se}\cdots\text{F}}$ for **5c** was 0.49 Å smaller in method II than in method I. For the other compounds, the decrease in $r_{\text{Se}\cdots\text{F}}$ was $\sim 0.13\text{--}0.28$ Å. Although the effect of electron correlation is significant, it is notable that the values of $r_{\text{Se}\cdots\text{F}}$ obtained at the Hartree–Fock level ($\sim 2.92\text{--}3.25$ Å in method I) were already smaller than the sum of the van der Waals radii (3.37 Å).²⁸ Therefore, electron correlation may not be an essential factor for formation of the nonbonded Se...F interactions.

For the case of **5f** (X = Me), the relative energies of conformer A to conformers B and C were -0.2 and $+0.0$ kcal/mol, respectively, in method II, suggesting that the three conformers exist in solution for **1f**. The most stable was found to be conformer C. This unique character of **5f** (= **1f**) may be due to dual weak intramolecular interactions, i.e., C–H...Se²⁹ and C–H...F hydrogen bonds, as shown in Figure 5. The obtained H...Se and H...F nonbonded distances were 2.89 and 2.24 Å, respectively, which were significantly shorter than the corresponding sum of the van der Waal radii (3.10 and 2.67 Å, respectively).²⁸

Structural parameters of conformer A ($r_{\text{Se}\cdots\text{F}}$, $\angle\text{F}\cdots\text{Se}-\text{X}$, and $\omega_{\text{Ar}-\text{C}}$) obtained for **5a–f** indicated the distinct tendency that the shorter the nonbonded Se...F atomic distance ($r_{\text{Se}\cdots\text{F}}$) is, the more linear the nonbonded F...Se–X angle ($\angle\text{F}\cdots\text{Se}-\text{X}$) is and the smaller the dihedral angle between the aromatic plane and the C–F bond ($\omega_{\text{Ar}-\text{C}}$) is. The linear propensity of the Se...F interactions suggested a major contribution from the orbital interaction between the antibonding orbital of the Se–X bond ($\sigma_{\text{Se}-\text{X}}^*$) and the lone pair of F (n_{F}) on the stability. Indeed, the mixing of $\sigma_{\text{Se}-\text{X}}^*$ and n_{F} was apparent for the case of **5a** as graphically shown in Figure 6. Such $n \rightarrow \sigma_{\text{Se}-\text{X}}^*$ orbital interactions have also been suggested for the corresponding Se...N⁸ and Se...O¹¹ interactions as the major stabilization factor.

To evaluate the magnitude of the $n_{\text{F}} \rightarrow \sigma_{\text{Se}-\text{X}}^*$ orbital interaction, NBO deletion analysis,²⁷ which should allow quantitative estimation of the total energy due to the orbital interactions between two specific atoms or groups in a molecule by deleting the Fock matrix elements, was applied to conformers A of **5a–f**. The obtained stabilization energies due to the orbital

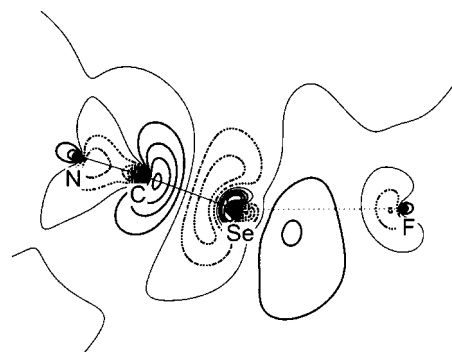


Figure 6. Contour map of LUMO+3 for conformer A of **5a** (X = CN) at the HF/6-31G(d,p) level by use of Huzinaga's 43321/4321/311 basis sets for Se. The map was drawn at the plane on the Se, F, and N atoms with a line interval of 0.05. Thin solid lines mean intersection of the nodal surface.

interactions between the SeX moiety and the F atom (ΔE_{del} in Table 2) showed a significant magnitude of Se...F orbital interactions (1.0–3.5 kcal/mol). The values of Δq_{Se} and Δq_{F} , which indicate electron flow in the formation of the nonbonded Se...F interaction, suggested that the F atom slightly donates electrons to the SeX moiety. Thus, the character of the $n_{\text{F}} \rightarrow \sigma_{\text{Se}-\text{X}}^*$ orbital interaction was supported theoretically.³⁰

Mechanisms of Se...F Interaction. Stabilization mechanisms for weak nonbonded interactions generally involve several physical factors, such as electrostatic, orbital (charge-transfer), and dispersion interactions. Their relative contributions depend on the interaction systems. For the case of the Se...F interaction observed for **1e** (the Se–Se...F interaction), the electrostatic character is presumably not important as revealed by the negligible solvent effects, while the orbital character may be significant as suggested by the large $J_{\text{Se}\cdots\text{F}}$ coupling constant estimated for conformer A of **1e** [$J_{\text{Se}\cdots\text{F}}(\text{A}) = 73$ Hz in CD₂Cl₂ and 81 Hz in CD₃CN] and by the QC and NBO analyses on **5e**.

On the other hand, an electrostatic character may contribute to some extent for the Se...F interaction of **1a** (the NC–Se...F interaction) as suggested by the solvent effect on the $J_{\text{Se}\cdots\text{F}}$ coupling constant. However, the contribution from orbital interactions should be more important, based on the large value of $J_{\text{Se}\cdots\text{F}}$ estimated for conformer A of **1a** [$J_{\text{Se}\cdots\text{F}}(\text{A}) = 120$ Hz in CD₂Cl₂] and the results of the QC and NBO analyses of **5a** (Table 2 and Figure 6). Since the QC calculation result (i.e., ΔE_{AB}) in vacuo almost quantitatively reproduced the fitting result (i.e., $H_{\text{Se}\cdots\text{F}}$) that was based on experimental observations in solution, the solvent effect may be rather small. Therefore, the orbital character would be predominant for stabilization of the NC–Se...F interaction.

Table 2 shows that the relative electronic energy (ΔE_{AB}) and Se...F atomic distance ($r_{\text{Se}\cdots\text{F}}$) of conformer A significantly change depending on the calculation methods (method I vs method II). Since the B3LYP method incorporates the effect of electron correlation more efficiently, the results suggested that the contribution from dispersion forces may also be involved for the attractive nature of nonbonded Se...F interactions.

Conclusions

By means of data fitting of the nuclear spin coupling constant between Se and F ($J_{\text{Se}\cdots\text{F}}$) observed for **1a** and **1e** at various

(28) Bondi, A. J. *Phys. Chem.* **1964**, *68*, 441–451.

(29) (a) Iwaoka, M.; Tomoda, S. *J. Am. Chem. Soc.* **1994**, *116*, 4463–4464. (b) Iwaoka, M.; Komatsu, H.; Tomoda, S. *Bull. Chem. Soc. Jpn.* **1996**, *69*, 1825–1826. (c) Narayanan, S. J.; Sridevi, B.; Chandrashekar, T. K.; Vij, A.; Roy, R. *Angew. Chem., Int. Ed. Engl.* **1998**, *37*, 3394–3397. (d) Michalczuk, R.; Schmidt, J. G.; Moody, E.; Li, Z.; Wu, R.; Dunlap, R. B.; Odom, J. D.; Silks, L. A. *Angew. Chem., Int. Ed. Engl.* **2000**, *39*, 3067–3070.

(30) According to ref 16, the value of ΔE_{del} was 0.0 kcal/mol for **5f**. The discrepancy between the results of ref 16 and this work ($\Delta E_{\text{del}} = 1.6$ kcal/mol for **5f**) may be ascribed to the difference in the basis sets employed.

temperatures to the rapid equilibrium model (Figure 1), stabilization energies of the nonbonded Se \cdots F interactions ($H_{\text{Se}\cdots\text{F}}$) were estimated as 1.23 kcal/mol for **1a** (in CD₂Cl₂) and 0.85 and 0.83 kcal/mol for **1e** (in CD₂Cl₂ and CD₃CN, respectively). The stabilization energies were significantly smaller than the corresponding Se \cdots N⁸ and Se \cdots O¹¹ interactions, being consistent with the lower electron-donating ability of F lone pairs. The negligible solvent effect observed for **1e** suggested little electrostatic nature of the Se \cdots F interaction despite the high electronegativity of F. On the other hand, a small solvent effect was observed for **1a**, suggesting the Se \cdots F interaction has a slight electrostatic character. The solvation site, however, may be the SeCN moiety rather than the CH₂F moiety.

As for the major mechanism of the nonbonded Se \cdots F interactions, the n_F \rightarrow $\sigma^*_{\text{Se}-\text{X}}$ orbital interaction was strongly suggested on the basis of the observed large $J_{\text{Se}\cdots\text{F}}$ coupling constants as well as the results obtained from QC calculations and the NBO analysis. The stabilization mechanism is essentially the same as the previously investigated Se \cdots N⁸ and Se \cdots O¹¹ interactions, although the nucleophilicity of F is much lower than those of N and O. Therefore, the strong electrophilicity of a divalent organic selenium as well as the weak, but distinct, electron-donating character of the lone pairs of organic fluorides¹⁵ can be concluded.

Experimental Section

General Procedures. Commercially available organic and inorganic reagents were used without further purification. Tetrahydrofuran (THF) was dried over sodium wire and was distilled under nitrogen. Dichloromethane (CH₂Cl₂) was dried over calcium hydride and was distilled under nitrogen before use. Methanol (MeOH) was distilled under nitrogen. Other organic solvents were used without purification. Gel-permeation chromatography was carried out by using a JAI LC-908 system equipped with JAIGEL-H columns (chloroform as eluent). ¹H (500 MHz), ¹³C (125.65 MHz), ¹⁹F (470.40 MHz), and ⁷⁷Se (95.35 MHz) NMR spectra were measured on a Jeol α 500 spectrometer in CDCl₃ containing tetramethylsilane as an internal standard for ¹H and ¹³C NMR. For ¹⁹F NMR, fluorobenzene (δ -113.0 ppm) was added as an internal standard. For ⁷⁷Se NMR, dimethyl selenide (δ 0 ppm) in CDCl₃ was used as an external standard. $J_{\text{Se}\cdots\text{F}}$ coupling constants of **1** and **4** were measured from the expanded ¹H-decoupled ⁷⁷Se NMR spectra in appropriate solvents at various temperatures. The temperatures were not corrected.

Bis[2-(fluoromethyl)phenyl] Diselenide (1e). According to the literature method,¹⁸ the well-ground 2:3 (w/w) mixture of potassium fluoride and calcium fluoride (from an artificial source) (5.20 g, 35.8 mmol of KF) was activated for 5 h at 150 °C under reduced pressure (0.1 mmHg). The mixture was added to the solution of bis[2-(chloromethyl)phenyl] diselenide¹⁷ (1.51 g, 3.67 mmol) in butyronitrile (10 mL) under nitrogen. After refluxing for 85 h, the reaction mixture was filtered. The filtration residue was washed with ether, and the ether layer was combined with the filtrate. After evaporation, the resulting crude product was purified by silica-gel column chromatography (hexane-CH₂Cl₂). Product **1e** was obtained in 47% yield (0.65 g) as yellow crystals. Spectral data for **1e**: ¹H NMR δ 7.65 (d, J = 7.6 Hz, 2H), 7.41 (d, J = 7.6 Hz, 2H), 7.35 (t, J = 7.6 Hz, 2H), 7.25 (t, J = 7.6 Hz, 2H), 5.42 (d, J_{HF} = 47.9 Hz, 4H); ¹³C NMR δ 138.0 (d, J_{CF} = 16.2 Hz), 135.3, 130.0 (d, J_{CF} = 4.1 Hz), 129.5 (d, J_{CF} = 1.7 Hz), 129.1, 128.1 (d, J_{CF} = 8.8 Hz), 84.0 (d, J_{CF} = 169.7 Hz); ¹⁹F NMR δ -208.1 (t, J_{HF} = 47.9 Hz); ⁷⁷Se NMR δ 437.3 (d, J_{SeF} = 23.6 Hz). Anal. Calcd for C₁₄H₁₂F₂Se₂: C, 44.70; H, 3.22. Found: C, 44.64; H, 3.37.

2-(Fluoromethyl)benzeneselenenyl Chloride (1b). Compound **1e** (19.1 mg, 0.05 mmol) was dissolved in dry THF (2 mL) under nitrogen,

and sulfonyl chloride (4.8 μ L, 0.06 mmol) was added to the solution. After having stirred for 1.5 h at 40 °C, the reaction mixture was concentrated under reduced pressure. The resulting crude product (brown oil) contained **1b** (79%), **1e** (16%), and an unknown byproduct (5%) according to the integration of ¹H NMR. Further purification of **1b** could not be performed because of the high reactivity of **1b**. Spectral data for **1b**: ¹H NMR δ 7.90 (d, J = 7.9 Hz, 1H), 7.51 (d, J = 7.9 Hz, 1H), 7.45 (t, J = 7.9 Hz, 1H), 7.42 (t, J = 7.9 Hz, 1H), 5.65 (d, J_{HF} = 49.2 Hz, 2H); ¹³C NMR δ 138.0 (d, J_{CF} = 17.7 Hz), 134.8, 131.5 (d, J_{CF} = 2.6 Hz), 130.6, 129.7 (d, J_{CF} = 0.8 Hz), 128.0 (d, J_{CF} = 8.6 Hz), 84.3 (d, J_{CF} = 167.6 Hz); ¹⁹F NMR δ -205.2 (t, J_{HF} = 49.2 Hz); ⁷⁷Se NMR δ 978.5 (d, J_{SeF} = 80.1 Hz).

2-(Fluoromethyl)phenylselenenyl Cyanate (1a). Compound **1b**, prepared from **1e** (193 mg, 0.51 mmol), was dissolved in dry THF (20 mL) under nitrogen. Cyanotrimethylsilane (175 μ L, 1.32 mmol) was added to the solution. After 1 h, the reaction mixture was concentrated under reduced pressure. Product **1a** was obtained in 80% yield (176 mg) as a colorless oil from the residue by silica-gel column chromatography (hexane-CH₂Cl₂) followed by gel-permeation chromatography. Spectral data for **1a**: ¹H NMR δ 7.86 (d, J = 7.0 Hz, 1H), 7.47 (d, J = 4.2 Hz, 1H), 7.45-7.41 (m, 2H), 5.52 (d, J_{HF} = 46.9 Hz, 2H); ¹³C NMR δ 137.0 (d, J_{CF} = 17.9 Hz), 134.0, 130.9 (d, J_{CF} = 1.9 Hz), 130.0, 129.6 (d, J_{CF} = 8.3 Hz), 123.1, 101.4 (d, J_{CF} = 6.4 Hz), 84.1 (d, J_{CF} = 168.6 Hz); ¹⁹F NMR δ -204.3 (t, J_{HF} = 46.9 Hz); ⁷⁷Se NMR δ 288.6 (d, J_{SeF} = 84.2 Hz). Anal. Calcd for C₈H₆FNSe: C, 44.88; H, 2.82; N, 6.54. Found: C, 44.59; H, 2.89; N, 6.52.

2-(Fluoromethyl)benzeneselenenyl Bromide (1c). Compound **1e** (19.0 mg, 0.05 mmol) was dissolved in CH₂Cl₂ (2 mL) under nitrogen, and bromine (2.59 μ L, 0.05 mmol) was added to the solution. After 15 min, the reaction mixture was evaporated. Product **1c** was almost quantitatively obtained as a dark brown oil. Because of the labile nature of **1c**, purification was not performed. Spectral data for **1c**: ¹H NMR δ 7.93 (d, J = 7.6 Hz, 1H), 7.52 (d, J = 7.6 Hz, 1H), 7.47 (t, J = 7.6 Hz, 1H), 7.37 (t, J = 7.6 Hz, 1H), 5.68 (d, J_{HF} = 47.4 Hz, 2H); ¹³C NMR δ 139.3 (d, J_{CF} = 16.9 Hz), 137.0, 131.1, 129.6 (d, J_{CF} = 3.0 Hz), 128.5 (d, J_{CF} = 4.3 Hz), 128.0 (d, J_{CF} = 9.5 Hz), 84.2 (d, J_{CF} = 168.6 Hz); ¹⁹F NMR δ -208.0 (t, J_{HF} = 47.4 Hz); ⁷⁷Se NMR δ 801.0 (d, J_{SeF} = 43.1 Hz).

2-(Fluoromethyl)benzeneselenenyl Phenyl Sulfide (1d). Compound **1e** (19.2 mg, 0.05 mmol) was dissolved in CH₂Cl₂ (2 mL). Pyridine (2 drops) and benzenethiol (26.1 μ L, 0.25 mmol) were added to the solution. After 2.5 h, the reaction mixture was concentrated under reduced pressure to afford a yellow oil, which contained **1d**, **1e**, and PhSSPh. The yield of **1d** was 30% according to the integration of ¹H NMR. Due to the disproportionation of **1d**, purification could not be performed. Spectral data for **1d**: ¹H NMR δ 7.78 (d, J = 7.3 Hz, 1H), 7.51-7.21 (m, 8H), 5.48 (d, J_{HF} = 49.1 Hz, 2H); ¹³C NMR δ 136.7 (d, J_{CF} = 16.4 Hz), 136.3, 132.5, 130.3, 129.7 (d, J_{CF} = 1.3 Hz), 129.0, 128.5 (d, J_{CF} = 7.5 Hz), 128.4, 127.7, 127.5, 83.9 (d, J_{CF} = 167.6 Hz); ¹⁹F NMR δ -206.3 (t, J_{HF} = 49.1 Hz); ⁷⁷Se NMR δ 499.7 (d, J_{SeF} = 38.7 Hz).

2-(Fluoromethyl)phenyl Methyl Selenide (1f). Compound **1e** (193 mg, 0.51 mmol) and methyl iodide (0.2 mL, 3.2 mmol) were dissolved in MeOH (2 mL) under nitrogen, and sodium borohydride was added to the solution until the yellow color disappeared. After 2 h, the reaction mixture was poured into aqueous NaHCO₃ (10 mL) and was extracted with ether. Product **1f** was obtained as a colorless oil (162 mg, 78%) after purification by gel-permeation chromatography. Spectral data for **1f**: ¹H NMR δ 7.48 (d, J = 7.0 Hz, 1H), 7.39 (d, J = 7.0 Hz, 1H), 7.30-7.23 (m, 2H), 5.49 (d, J_{HF} = 47.7 Hz, 2H), 2.32 (s, 3H); ¹³C NMR δ 136.8 (d, J_{CF} = 17.6 Hz), 131.9 (d, J_{CF} = 3.8 Hz), 131.2, 129.4 (d, J_{CF} = 2.5 Hz), 128.4 (d, J_{CF} = 7.5 Hz), 126.6, 84.1 (d, J_{CF} = 167.6 Hz), 7.7; ¹⁹F NMR δ -208.1 (t, J_{HF} = 47.7 Hz); ⁷⁷Se NMR δ 161.1 (d, J_{SeF} = 22.7 Hz). Anal. Calcd for C₈H₉FSe: C, 47.31; H, 4.47. Found: C, 47.01; H, 4.41.

Sodium [2-(Fluoromethyl)phenyl]seleno(trimethoxy)borate (1g).

Compound **1g** was generated in an NMR sample tube by the reaction of **1e** with excess amounts of sodium borohydride in CD₃OD.¹⁹ Although ¹H and ¹³C NMR spectra of the reaction mixture were significantly complicated, the formation of **1g** was characterized by ¹⁹F and ⁷⁷Se NMR spectra. 6*H*,12*H*-Diseleno[*b*,*f*][1,5]diselenocin^{29a,b} was detected as a major byproduct during the prolonged measurement of the NMR spectra. Spectral data for **1g**: ¹⁹F NMR δ -217.6 (t, *J*_{HF} = 49.3 Hz); ⁷⁷Se NMR δ -24.1 (s).

2-(Trifluoromethyl)phenylselenenyl Cyanate (4a). 2-(Trifluoromethyl)aniline (3.32 g, 20.6 mmol) was suspended in 6 M HCl (40 mL) at 0 °C, and 3 M NaNO₂ (8 mL, 24 mmol) was added to the mixture dropwise. After 1 h, a saturated aqueous solution of sodium acetate was added dropwise until the pH of the reaction solution reached about 6. Then the mixture was poured into aqueous potassium selenocyanate (3.70 g, 20.5 mmol). The resulting mixture was extracted with ether. After purification by silica-gel column chromatography (hexane-CH₂-Cl₂), **4a** was obtained as a brown oil (4.40 g, 85%). Spectral data for **4a**: ¹H NMR δ 7.97 (d, *J* = 7.7 Hz, 1H), 7.74 (d, *J* = 7.7 Hz, 1H), 7.59 (t, *J* = 7.7 Hz, 1H), 7.52 (t, *J* = 7.7 Hz, 1H); ¹³C NMR δ 133.9, 133.6, 129.8 (q, *J*_{CF} = 31.6 Hz), 129.2, 127.6 (q, *J*_{CF} = 5.4 Hz), 123.3 (q, *J*_{CF} = 274.2 Hz), 121.0, 100.7 (q, *J*_{CF} = 4.7 Hz); ¹⁹F NMR δ -60.6 (s); ⁷⁷Se NMR δ 341.7 (q, *J*_{SeF} = 63.2 Hz).

Bis[2-(trifluoromethyl)phenyl] Diselenide (4e). Compound **4a** (1.05 g, 4.2 mmol) and NaOH (7.12 g, 0.18 mol) were dissolved in methanol (50 mL), and the mixture was stirred at room temperature for 24 h. The reaction mixture was added to water and was extracted with CH₂-Cl₂. Product **4e** was obtained as yellow crystals (0.64 g, 68%) after purification by silica-gel column chromatography (hexane). Compound **4e** was known in the literature.³¹ Spectral data for **4e**: ¹H NMR δ 7.88 (d, *J* = 7.7 Hz, 2H), 7.60 (d, *J* = 7.7 Hz, 2H), 7.39 (t, *J* = 7.7 Hz, 2H), 7.31 (t, *J* = 7.7 Hz, 2H); ¹³C NMR δ 133.6, 132.7, 129.5 (q, *J*_{CF} = 30.3 Hz), 128.5, 127.5, 126.6 (q, *J*_{CF} = 7.6 Hz), 123.9 (q, *J*_{CF} = 274.0 Hz); ¹⁹F NMR δ -60.1 (s); ⁷⁷Se NMR δ 454.0 (q, *J*_{SeF} = 53.0 Hz).

2-(Trifluoromethyl)phenyl Methyl Selenide (4f). Compound **4a** (527 mg, 2.1 mmol) and methyl iodide (0.33 mL, 5.3 mmol) were dissolved in MeOH (6 mL) under nitrogen, and sodium borohydride was added to the solution until the yellow color disappeared. After 2 h, the reaction mixture was added to aqueous NaHCO₃ and was extracted with ether. Product **4f** was obtained as a colorless oil (417 mg, 83%) after purification by gel-permeation chromatography. Spectral

data for **4f**: ¹H NMR δ 7.59 (d, *J* = 7.8 Hz, 1H), 7.47 (d, *J* = 7.8 Hz, 1H), 7.39 (t, *J* = 7.8 Hz, 1H), 7.24 (t, *J* = 7.8 Hz, 1H), 2.34 (s, 3H); ¹³C NMR δ 132.0, 131.5, 131.0, 130.1 (q, *J*_{CF} = 30.4 Hz), 126.7 (q, *J*_{CF} = 5.2 Hz), 125.7, 124.1 (q, *J*_{CF} = 272.0 Hz), 7.5; ¹⁹F NMR δ -61.7 (s); ⁷⁷Se NMR δ 217.7 (q, *J*_{SeF} = 48.4 Hz).

Sodium [2-(Trifluoromethyl)phenyl]seleno(trimethoxy)borate (4g). Compound **4g** was generated in an NMR sample tube by the reaction of **4e** with excess amounts of sodium borohydride in CD₃-OD.¹⁹ Formation of **4g** was unambiguously characterized by NMR spectra. Spectral data for **4g**: ¹H NMR δ 7.82 (t, *J* = 8.3 Hz, 1H), 7.28 (t, *J* = 8.3 Hz, 1H), 6.88 (t, *J* = 8.3 Hz, 2H); ¹³C NMR δ 142.1, 140.6, 134.2 (q, *J*_{CF} = 26.4 Hz), 130.3, 126.5 (q, *J*_{CF} = 5.3 Hz), 126.5 (q, *J*_{CF} = 273.5 Hz), 122.2; ¹⁹F NMR δ -63.6 (s); ⁷⁷Se NMR δ 69.5 (q, *J*_{SeF} = 15.6 Hz).

Data Fitting. The values of *J*_{Se...F} for **1a** and **1e** were measured in CD₂Cl₂ and CD₃CN at various temperatures from the expanded ¹H-decoupled 95.35 MHz ⁷⁷Se NMR spectra with a digital resolution of 0.15 Hz. The data obtained were fitted to eqs 1–3 by using KaleidaGraph version 3.08 (Synergy Software, Reading, PA), in which the Levenberg–Marquardt algorithm³² was employed for the nonlinear least-squares method.

QC Calculations and the NBO Analysis. All computational calculations were carried out by using Gaussian 94 and 98 programs^{23,24} installed on DEC Alpha21164A Unix workstations. Stable conformers of **5a–f** were first sought by changing the two dihedral angles along the Ar–SeX and Ar–CH₂F bonds independently with an interval of 30° at the HF/3-21G(d) level. The obtained conformers (conformers A, B, C, etc.) were fully optimized at the HF/6-31G(d,p) (method I) and B3LYP/6-31G(d,p) (method II) levels by use of Huzinaga's 43321/4321/311 basis sets²⁵ without any restrictions. The single-point energies were then calculated by applying the density functional theory at the B3LYP/6-31G(d,p) level.²⁶ Zero-point energies (ZPE) calculated at the appropriate level were not scaled. NBO deletion analysis²⁷ was performed with standard parameters at the HF/6-31G(d,p) level. The contour map of LUMO+3 for **5a** (Figure 6) was drawn by using a homemade program.

Acknowledgment. This work was supported by Grants in Aid for Scientific Research 11120210 and 10133207 from the Ministry of Education, Science and Culture, Japan.

JA016348R

(31) McKillop, A.; Koyunçu, D.; Krief, A.; Dumont, W.; Renier, P.; Trabelsi, M. *Tetrahedron Lett.* **1990**, *31*, 5007–5010.

(32) Marquardt, D. W. *J. Soc. Ind. Appl. Math.* **1963**, *11*, 431–441.